DEVELOPMENT OF COS-THETA Nb_3Sn DIPOLE MAGNETS FOR VLHC*

A.V. Zlobin†, G. Ambrosio, N. Andreev, E. Barzi, D. Chichili, V.V. Kashikhin,
P.J. Limon, I. Terechkine, S. Yadav, R. Yamada, FNAL, Batavia, IL 60510, USA

Abstract

This paper describes the double aperture dipole magnets developed for a VLHC based on Nb_3Sn superconductor, a cos-theta coil, cold and warm iron yokes, and the wind-and-react fabrication technique. Status of the model R&D program, strand and cable and other major component development are also discussed.

1 INTRODUCTION

A feasibility study performed recently at Fermilab for a post-LHC Very Large Hadron Collider (VLHC) adopted a staged scenario with low and high field rings in the 233 km tunnel [1]. The stage 2 (VLHC-2) ring with 10 T Nb_3Sn magnets will collide protons with a center of mass energy of 175 TeV. In order to provide both flat and round beam optics in the interaction regions, magnets with a vertical bore arrangement are required. A Nb_3Sn dipole based on the common coil design and the react-and-wind fabrication technique was, therefore, chosen as the baseline arc dipole magnet. This approach is regarded as the most innovative and cost effective.

An alternative approach is based on Nb_3Sn cos-theta coils that need a smaller coil cross-section with respect to block-type coils with the same aperture and field. In addition, these coils allow both horizontal and vertical bore arrangements and a smaller distance between the apertures, thereby reducing yoke and magnet size, weight and cost. However, due to the small bending radii, cos-theta coils are required to use the wind-and-react technique in order to avoid a large degradation of the cable critical current during coil winding.

Both design approaches are being studied at Fermilab in order to provide a solid justification for the magnet design for VLHC-2 [2]. This paper presents the results of a design study of double-aperture dipole magnets based on the Nb_3Sn cos-theta coil.

2 MAGNET DESIGN

The coil cross section is shown in Fig. 1. The bore diameter is 43.5 mm, but it can be easily varied within the 40-50 mm range with small cross-section adjustment. Each half-coil consists of two layers with 24 turns, and has two pole inserts and eight wedges, which allow minimizing low order field harmonics.

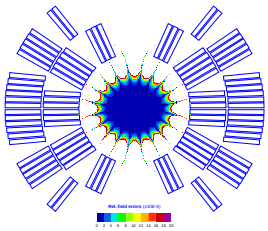

Figure 1: Coil geometry and field quality.

The coil utilizes a keystone Rutherford-type cable made of 28 Nb_3Sn strands 1 mm in diameter. The width of the bare cable is 14.24 mm, the thickness is 1.800 mm, the keystone angle is 0.91 degree and the packing factor is 88%. The thickness of the cable insulation is 0.25 mm. Both inner and outer layers are wound from one piece of cable without an inter-layer splice.

The cross sections of the double bore dipole magnets based on the cos-theta Nb_3Sn coils described above, with cold and warm iron yokes and with horizontal and vertical bore arrangements are shown in Figure 2.

In design (a) the two coils are placed side by side in a cold iron yoke with an aperture separation of 180 mm. This parameter can be varied within the 160-200 mm range for the same iron OD without noticeable effect on the field quality. The yoke is vertically split into three pieces to allow assembly of two coils in the common yoke. The coil prestress is provided by the yoke and the

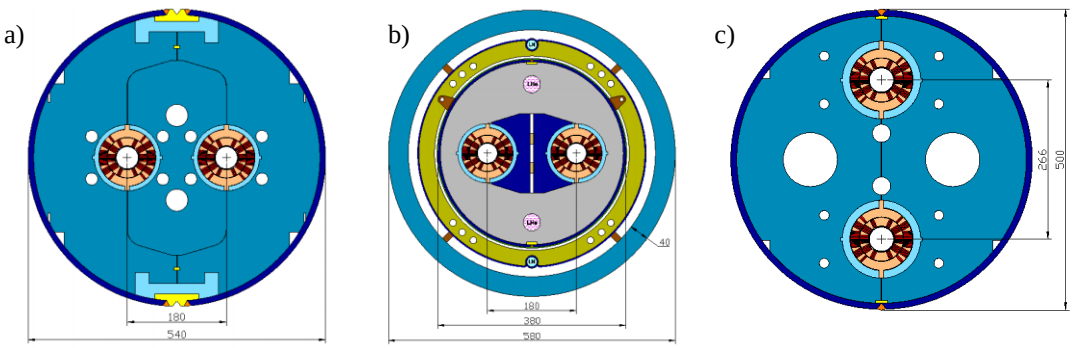

Figure 2: Double bore dipole magnets based on the cos-theta Nb_3Sn coil, cold (a, c) and warm (b) iron yoke with horizontal (a, b) and vertical (c) bore arrangement.

* Work supported by the U.S. Department of Energy.
† zlobin@fnal.gov

stainless steel skin. Since two horizontal components of the Lorentz force acting on the left and right sides of both coils are compensated inside the cold mass, a 10 mm thick skin is sufficient to provide an effective coil support. An open gap minimizes the reduction of coil prestress after cool down. In order to reduce the effect of gap variation on the field quality, the yoke split is partially parallel to the flux lines so that it crosses only a small amount of peripheral lines in the vertical plane. The iron saturation effect is suppressed by introducing special holes and by optimizing the yoke outer diameter.

In design (b) the warm iron is remote from the coils far enough to accommodate such cryostat elements as the support system, the thermal shield and the vacuum vessel. The two coils are placed inside the cylindrical yoke with an aperture separation of 180 mm as in design (a). The thick aluminum rings and stainless steel inserts provide the coil prestress and mechanical support. The cold mass skin is thin since it is not a part of the coil support structure. The yoke inner radius and thickness were optimized with respect to field quality, fringe fields, iron cross-section and considerations related to the cryostat design. The iron saturation effect in the warm yoke design is small. A magnetic coupling between the two coils results in a large quadrupole component of the field. It is compensated in each aperture by the geometrical quadrupole component of opposite sign generated by introducing a small left-right asymmetry in coil block position.

In design (c) the two coils are placed inside the cold yoke one on top of the other. To reduce the negative magnetic coupling between them to an acceptable level a minimum aperture separation of 266 mm is required. In order to minimize the size of the cold mass, the yoke is divided in two parts – cold and warm (the latter is not shown in Figure 2c). The cold part of the yoke is vertically split in two pieces for assembly and pre-stressing the coils. The coil prestress is provided by the yoke and the 20-mm thick stainless steel skin. The skin thickness is a factor of two thicker than in design (a) since the horizontal components of Lorentz force acting on each coil are not compensated but added. In order to minimize prestress reduction after cool down, the gap stays open. The warm part of the yoke is remote in order to accommodate the cryostat elements as in design (b). The iron saturation effect in this design is suppressed using holes in the iron, and optimizing the cold and warm yoke inner and outer radii.

Designs (b) and (c) require a proper alignment of the cold mass inside the warm yoke to reduce the force imbalance and the effect on the field quality. Analysis shows that the alignment requirements are quite modest and can be easily met.

The mechanical analysis shows [3] that in all the above designs the coil is under compression, but that the stress never exceeds 150 MPa, still acceptable for a strain sensitive Nb_3Sn cable. The coil bore deformations are small, less than 100 μm, and all structural elements work in the elastic regime.

3 MAGNET PARAMETERS

The main parameters of the dipole magnets described above are summarized in Table I. All the designs meet the VLHC-2 requirements. The magnet designs with warm yoke allow a significant reduction in size without noticeable degradation in performance.

Table I: Calculated magnet parameters.

Bore arrangement	**Horizontal**		**Vertical**
Yoke design	Cold	Warm	Cold+Warm
Aperture, mm	43.5	43.5	43.5
Aperture separation, mm	180	180	266
Iron yoke OD, mm	520	580	564+710
Iron yoke area, cm^2	1722	679	1378+327
B_{max}, T	12.05	11.34	11.59
I_{max}, kA	21.9	24.0	22.3
B/I @11T, T/kA	0.56	0.47	0.52
Stored energy @11T, kJ/m	2×260	2×294	2×277
Inductance @11T, mH/m	2×1.34	2×1.08	2×1.23

The values of B_{max} and I_{max} were calculated for Nb_3Sn strands with Cu/nonCu=0.85:1 and J_c=2.0 kA/mm^2 at 12T and 4.2K. Assuming a 10% I_c degradation these designs can provide B_{max}~10-11.5 T using present Nb_3Sn strand. A B_{nom}~10-11 T with 10-15% margin will be achieved using R&D strands with J_c=3.0 kA/mm^2 and Cu/nonCu=1.2, which is required for quench protection.

The calculated geometrical harmonics and RMS spread for ±50 μm random displacements of coil blocks are summarized in Table II.

Table II: Geometrical Harmonics at 1 cm radius, 10^{-4}.

Har-monic #	**Horizontal**		**Vertical**	**RMS ($\sigma_{a,b}$)**
	Cold yoke, bn	**Warm yoke bn**	**Cold yoke bn**	
2	-	0.000	-	1.198
3	0.000	0.000	0.000	0.564
4	-	0.000	-	0.279
5	0.000	0.001	-0.000	0.103
6	-	-0.012	-	0.047
7	0.000	-0.011	-0.006	0.021
8	-	0.031	-	0.008
9	-0.091	-0.130	-0.067	0.005
10	-	-0.011	-	0.001

The iron saturation effect on the low order harmonics in the operating field range 1-10 T is effectively suppressed down to ±0.5 units by optimizing the yoke and correction hole sizes. The coil magnetization effect at low fields is large (b_3=–20-25 units at B=1 T) with present Nb_3Sn strands having a large effective filament diameter d_{eff}~100 μm [4]. It can be reduced by a factor of seven using a simple passive correction based on iron strips [5]. Further reduction could be achieved by reducing the d_{eff} in Nb_3Sn strands. Eddy current effects will be minimized using strands with a small filament twist pitch and optimizing the crossover resistance in the cable.

4 MAGNET DEVELOPMENT STATUS

Short model R&D. A Nb_3Sn cos-theta coil is the key element of all the designs. Coil fabrication technology uses the wind-and-react approach to avoid a large degradation of the cable critical current during winding. In order to simplify the technology and reduce the cost, new features were introduced in the fabrication process. Each half-coil is impregnated with a liquid ceramic binder and cured at 120C after winding to pre-form coils before reaction. Then the two half-coils are assembled, reacted and epoxy impregnated together. It allows easy coil handling, coil size and field quality control before the final magnet assembly, thereby avoiding expensive collars and a delicate collaring procedure.

To validate and optimize the coil and magnet designs, a model magnet program has been undertaken. It started with single-bore cold-yoke models [6] and later will be expended to double bore models. A first 1-m long model magnet was recently fabricated (see Figure 3) and now is being tested at Fermilab [7].

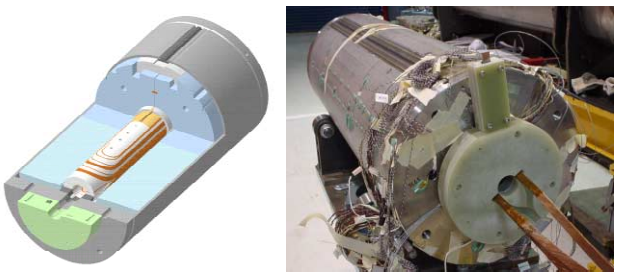

Figure 3: Short model 3D view and assembled cold mass.

Strand and cable. To reach the VLHC-2 nominal field, Nb_3Sn strands and cables must meet specific requirements. Nb_3Sn strands produced using Internal Tin (IT), Modified Jelly Roll (MJR), and Powder-in-Tube (PIT) processes were purchased and tested at Fermilab. The critical current density, J_c, of these strands was measured to be within 1900-2200 A/mm^2. It is controlled by the volumetric fraction of Nb_3Sn phase, the heat treatment schedule, and the flux pinning mechanisms. All these parameters are presently studied and optimized in order to reach the required Jc of 3000 kA/mm^2.

The strand magnetization and stability are driven by Jc and d_{eff}. For the strands produced using the most cost effective technologies such as IT or MJR, d_{eff} is ~100 μm. The PIT process provides it on the level of ~50 μm, but with a significant increase in the strand cost [4]. An optimization of the strand design and technology aiming at the reduction of d_{eff} in the high J_c strands is underway.

Strand plastic deformation during cabling, and reacted cable compression in the coil during magnet assembly and operation causes I_c degradation and variation of interstrand resistance. Cables with different packing factors were fabricated with and without a stainless steel core and short samples of virgin and extracted strands were tested. The studies show significant progress in developing of Nb_3Sn cables for accelerator magnets with Ic degradation less than 10% and high crossover resistance [8].

Insulation. The react-and-wind technique imposes demanding requirements on the coil insulation. The insulation must withstand a long heat treatment at high temperature (~700C) under high compression. The ceramic insulation meets these requirements and is being used in the short models with ceramic binder (CTD Inc.) which improves the insulation performance during coil manufacturing [6]. However, it is still rather expensive. An alternative is to use S-2 fiberglass, which is affordable but involves a lot of pre-processing. Both insulation systems are being extensively studied.

End parts. Cos-theta Nb_3Sn magnets use complicated 3D end parts that must withstand the heat treatment cycle without deformation and match the cable shape in the ends to avoid shorts. An optimization method for metallic end parts was developed and successfully tested [6]. Rapid prototyping techniques reduce time and cost of the optimization process for such end parts. Emerging technologies, such as water jet machining, promise a significant reduction of the end part cost by a factor of 2.5 and of the manufacturing time by a factor of 10.

5 CONCLUSION

The magnetic and mechanical designs of double aperture dipole magnets for a VLHC-2 based on a Nb_3Sn cos-theta coil with cold and warm iron yoke and horizontal and vertical bore arrangement were developed. All magnets meet the target requirements. A nominal field of 10 T with 15% margin will be achieved using future Nb_3Sn R&D strand. The accelerator field quality is provided in the entire field range of 1-10 T. The operating field range can be further expanded by reducing d_{eff} in Nb_3Sn strands and using simple passive correction. The chosen mechanical designs and the coil prestress level provides the coil mechanical stability in the fields up to 11-12 T. The first single-bore dipole model was fabricated and is being tested at Fermilab.

6 REFERENCES

[1] Design Study for a Staged Very Large Hadron Collider, Fermilab-TM-2149, June 4, 2001.
[2] V.V. Kashikhin, A.V. Zlobin, IEEE Trans. on Applied Superconductivity, v.11, No.1, March 2001, p. 2176.
[3] D.R. Chichili et al., IEEE Trans. on Applied Superconductivity, v.11, No.1, March 2001, p. 2288.
[4] E. Barzi et al., IEEE Trans. on Applied Superconductivity, v.11, No.1, March 2001, p.
[5] V.V. Kashikhin, A.V. Zlobin, IEEE Trans. on Applied Superconductivity, v.11, No.1, March 2001, p. 2058.
[6] D.R. Chichili, et al., IEEE Trans. on Applied Superconductivity, v.10, No.1, March 2000, p.2160.
[7] N. Andreev et al., "Field Quality of the Fermilab NB_3SN High Field Dipole model", this conference.
[8] E. Barzi et al., IEEE Trans. on Applied Superconductivity, v.11, No.1, March 2001, p. 2134.